



MacKenzie, L. E., Harvey, A. R. and McNaught, A. I. (2017) Spectroscopic oximetry in the eye: a review. *Expert Review of Ophthalmology*, 12(4), pp. 345-356.

There may be differences between this version and the published version. You are advised to consult the publisher's version if you wish to cite from it.

<http://eprints.gla.ac.uk/144297/>

Deposited on: 4 August 2017

Enlighten – Research publications by members of the University of Glasgow
<http://eprints.gla.ac.uk>

Spectroscopic oximetry in the eye: a review

ABSTRACT

Introduction: Non-invasive measurement of blood oxygen saturation via spectroscopic imaging has facilitated insights into the development and progression of a variety of ocular conditions, including retinal vascular occlusion, diabetic retinopathy and glaucoma. Major developments since the late 90s have been enabled by advancements in imaging technology, computational image analysis, and experimental methods.

Areas covered: We review the theory of spectroscopic oximetry, the ocular blood vessels targeted for oximetry, imaging systems used for oximetry, and oximetry validation methods. Important physiological and clinical insights provided by oximetry in the eye are detailed.

Expert commentary: Oximetry has revealed physiological norms and auto-regulatory effects in the retina, choroid, episcleral, and bulbar conjunctival blood vessels. Retinal oximetry has provided crucial insight into the development of diabetic retinopathy and glaucoma, and has enhanced the evaluation and treatment of retinal vessel occlusion. Commercially available retinal oximetry systems have enabled oximetry in the clinic. The development more sophisticated phantoms that resemble *in vivo* environments has oximetry validation in diverse oximetry applications. New insights into ocular physiology and disease are likely to be gleaned from future studies.

Keywords: oximetry, retina, autoregulation, diabetes, glaucoma, vessel occlusion, choroid, bulbar conjunctiva.

1. INTRODUCTION

Oximetry - the measurement of blood oxygen saturation (OS) – can be achieved non-invasively by measuring the spectrum of light absorbed by blood. This is achieved by imaging the eye at two or more wavelengths of light, and calibrating the OS to absorption of light by either (1) assuming standard normal OS values or (2), by combining information from many wavelengths into a sophisticated physical model incorporating the known spectral properties of blood with other biological and optical parameters.

Since the late 1950s, retinal oximetry has progressed from a photographic technique [1–3] through to the cutting edge of digital imaging technology with automated computational analysis.[4,5] Over the decades, retinal oximetry has revealed valuable insights into retinal physiology and metabolism under conditions such as flicker illumination,[6,7] dark adaptation,[8] hyperoxia,[4,9,10] and acute mild hypoxia.[11,12] Further, retinal oximetry has provided insights into the development and progression of ocular diseases such as diabetic retinopathy,[13–17] glaucoma,[18–22] and retinal vessel occlusion.[23–26] Recently, oximetry has allowed the understanding of the fundamental physiological oxygen dynamics of the bulbar conjunctival circulation,[27] the episcleral vessels,[27] and the choroidal circulation.[28]

38 From a patient's perspective, the experience of oximetry imaging in the eye is typically
39 indistinguishable from conventional retinal-fundus imaging because oximetry systems are typically
40 based on a modified conventional retinal-fundus cameras[4,11,16] or multi-wavelength scanning laser
41 ophthalmoscopes.[10,29] As such, a great deal of oximetry innovation has arisen from improved
42 image recording, computational image analysis, and the development of complimentary functional
43 oxygen-sensitive stress interventions that allow insight into OS under altered metabolic conditions.
44 These intervention tests include subjecting subjects to hyperoxia,[6,7] acute mild hypoxia,[11,12] or
45 altered light-exposure conditions.[6–8] As well as physiological and clinical insights, these intervention
46 tests help validate the accuracy of oximetry measurements.

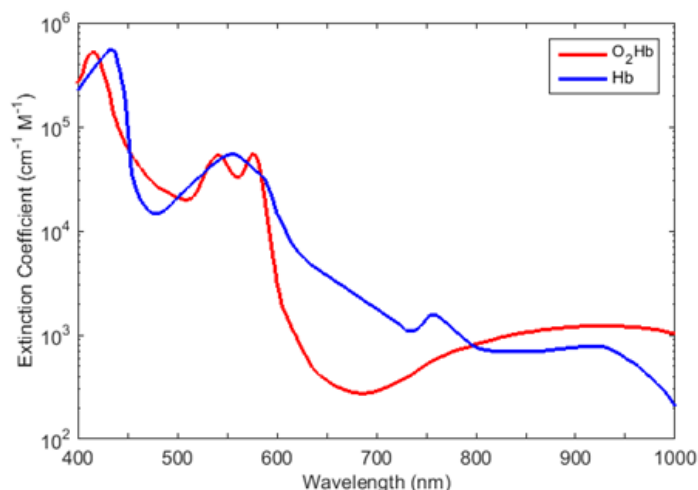
47 Invariably, advances in oximetric-imaging technology have provided new insights and applications.
48 In particular, the development of commercially available retinal oximetry devices with automated
49 analysis – such as the *Oxymap T1* (Oxymap ehf, Iceland) [4] and *Imedos* (Imedos Systems UG,
50 Germany)[16] retinal oximetry systems - have enabled oximetry in the clinic, allowing insights into
51 treatment of individual patients[24] and also enabling clinicians to build large datasets with high
52 statistical power. Additionally, the development of oximetry systems with capability for imaging with
53 greater temporal[11] and spatial resolution[29] enable development of novel techniques and fresh
54 insights by investigating OS of smaller blood vessels or by studying OS dynamics on a shorter timescale.
55 For example, snapshot multispectral imaging technology has enabled measurement of rapid oxygen
56 diffusion in the bulbar conjunctiva[27] and adaptive optics have enabled oximetry in small retinal
57 vessels, which are not typically studied due to their small diameters.[29]

58 This review focuses on the current technology and methods of spectroscopic oximetry, new
59 applications in spectroscopic oximetry of the eye, and the clinically useful ophthalmological insights
60 that have been consequently enabled.

61 **2. PRINCIPLE OF SPECTROSCOPIC OXIMETRY**

62 Spectroscopic oximetry is enabled by the distinct absorption spectra of oxygenated haemoglobin
63 (O_2Hb) and deoxygenated haemoglobin (Hb) as shown in Figure 1: partial oxygenation results in an
64 absorption spectrum that is a weighted average of these two spectra. This difference in optical
65 absorption can be clearly seen by eye for a low-volume sample of blood: highly oxygenated blood
66 appears bright red to the eye, whereas deoxygenated blood is much darker in appearance. Whilst this
67 difference in optical absorption is readily observed in *ex vivo* blood samples, it is highly challenging to
68 accurately quantify in the complex optical environment of the eye due to the influence of optical
69 scattering[30] and the uncertain absorption of light by variable background pigmentation.[9,31] There
70 are two approaches to spectroscopic oximetry measurement and analysis: two-wavelength oximetry
71 and multi-wavelength oximetry.

72



73

74

75

Figure 1. The absorption spectra of oxygenated haemoglobin (O₂Hb) and deoxygenated haemoglobin (Hb) at visible and near infra-red wavelengths.

76

2.1. Two-wavelength oximetry

77

78

79

80

81

82

83

84

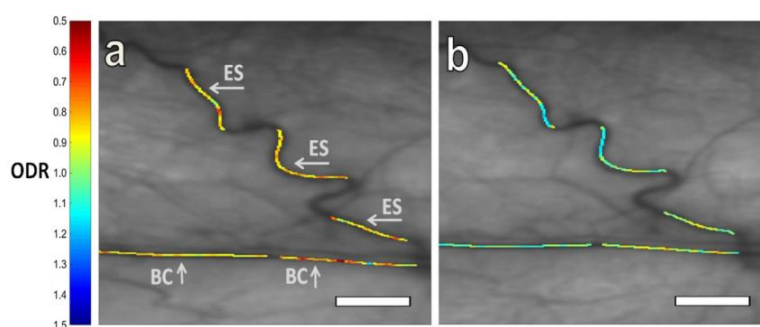
85

86

87

88

In two-wavelength oximetry, blood vessels are imaged at one OS-sensitive contrast wavelength, and another – typically OS-insensitive (isobestic) - wavelength. The optical transmission of blood vessels (T_λ) is measured at each wavelength, and the optical density (OD), defined as: $OD_\lambda = -\log(T_\lambda)$, is computed. From this, the optical density ratio (ODR), defined as $ODR = \frac{OD_{\lambda_{contrast}}}{OD_{\lambda_{isobestic}}}$, is calculated. If an isobestic wavelength is used, then for a blood vessel of a given diameter, ODR is theoretically directly proportional to blood oxygen saturation (verified experimentally in 1959)[1], and so ODR can be empirically related to OS by measuring ODR of blood vessels at two OS levels followed by calibration against a blood vessels of known oxygenation (i.e. using pulse oximetry or blood gas measurement). The theory of two-wavelength oximetry is based upon the simple Beer-Lambert law of light transmission, which neglects the effects of optical scattering that is incorporated into the modified Beer-Lambert law.[31] For visualisation purposes, ODR or OS is often overlaid as a colour map on images of blood vessels (see Figure 2 for an example).[4]



89

90

91

92

Figure 2. ODR colour-map of bulbar conjunctiva (BC) and episcleral (ES) vessels at (a) normoxia, and (b) acute mild hypoxia. Reproduced with permission from MacKenzie et al., (2016).[32]

93

94

The optimal transmission of a blood vessel for accurate oximetry is around 37%, [33] but, because the optical transmission of blood vessels varies according to several factors – including vessel

95 diameter - an optical transmission of between 10 % and 70 % has been found to work well.[33] For
96 retinal oximetry, the combination of 570 nm (isobestic) and 600 nm (contrast) wavebands has been
97 commonly adopted for retinal oximetry.[4,11,31] However, the optimal wavelength combinations
98 used for any oximetry study are dependent upon the calibre of vessels of interest and the efficiency
99 of optical imaging and detection systems.

100 Care is required in calibration of two-wavelength oximetry. In early retinal oximetry studies retinal
101 arterial OS was calibrated by comparison with *ex vivo* brachial-artery blood samples and blood gas
102 measurement.[1–3] Whilst useful for establishing relations between retinal arterial OS and systemic
103 arterial OS, *ex vivo* blood gas measurement is undesirable or not feasible and has been rendered
104 unnecessary by the advent of fingertip pulse oximetry which allows non-invasive estimation of
105 systemic arterial OS. However, calibrating arterial OS alone can lead to artefacts in estimated venous
106 OS. For example, it has been shown that ODR is dependent on blood vessel diameter and background
107 pigmentation; so two-wavelength oximetry requires calibration correction factors that are dependent
108 upon both background pigmentation and blood vessel diameter.[9,31] It has recently been postulated
109 that the laminar flow from multiple tributary branching veins, which leads to non-uniform blood
110 oxygenation within a vein may also degrade estimation of OS in retinal veins, which is based upon
111 homogeneous blood oxygenation. This significance of this factor requires experimental testing and
112 validation.[34]

113 Two-wavelength oximetry is the basis for the *Oxymap* and *Imedos* commercial retinal imaging
114 devices which have found considerable use in clinical applications (see Section 6).

115 **2.2. Multispectral oximetry techniques**

116 Multispectral oximetry is broadly defined as any oximetry technique that incorporates information
117 from three or more spectral wavebands to calculate OS.

118 **2.2.1. Three-wavelength oximetry**

119 The simplest form of multispectral oximetry, three-wavelength oximetry, [35] utilises two isobestic
120 wavelengths relatively close to each other on the wavelength spectra combined with a wavelength
121 providing oximetric contrast. From the two isobestic two wavelengths it is possible to quantify the
122 scattering of light by blood, and thus to appropriately alter estimation of blood-vessel transmission
123 via the modified Beer Lambert law.[35] Three-wavelength retinal oximetry was applied to the retinal
124 imaging with a scanning laser device by Delori in the 1980s and 1990s.[36,37] However, three
125 wavelength oximetry was somewhat difficult to apply because of the requirements of three
126 wavebands where blood exhibits similar optical scattering properties; this limited the range of useful
127 wavebands to which it can be applied.[33] As such, three-wavelength oximetry has tended to be
128 superseded by multispectral oximetry using four or more bands.

129 **2.2.2. Multispectral oximetry models**

130 Multispectral oximetry models enable estimation of OS by incorporating the optical transmission
131 of blood at a number of wavebands to isolate the absorption of light by blood and estimate or
132 compensate for other optical parameters, e.g. the scattering of light by blood and tissue, or the optical
133 absorption by melanin pigmentation. Typically, the transmissions of blood vessels are measured and
134 the experimental transmission compared to a theoretical model incorporating these parameters. This
135 enables direct estimation of OS without need of a reference value; i.e. multispectral algorithms are

136 “calibration free”. Thus, multispectral oximetry algorithms can provide quantitative oximetry in blood
137 vessels where OS levels have not yet been measured by other means (e.g. in the spinal cord)[38] or in
138 blood vessels that may be expected to be very different from physiological norms (e.g. studying
139 angiogenesis in tumour development)[39,40]. However, validation of estimated OS from multispectral
140 oximetry algorithms is normally desirable, and provides vital information for the wider field of
141 oximetry (see Section 5).

142 The number of wavebands incorporated into a multispectral imaging system varies greatly. Some
143 oximetry studies incorporate many wavebands (e.g. between 25 and 76 wavebands) into a
144 ‘hyperspectral’ model (see Table 1). Hyperspectral imaging offers the advantage a comprehensive
145 measurement of blood vessel transmission, but as a result of this, hyperspectral imaging systems are
146 typically burdened with a long acquisition time (i.e. > 1 minute) and high data volumes for a single
147 data set. Consequently, challenges arise from subject eye motion and alterations of OS of vessels
148 during hyperspectral measurement. Additionally, some wavebands may be sub-optimal for oximetry;
149 for example, blue wavelengths suffer from lower instrumental signal-to-noise ratios and high
150 absorption by melanin pigmentation, and auto-fluorescence from blood or other tissue. Imaging
151 spectrograph devices offer excellent spectral resolution and have been employed for spectroscopy of
152 the eye,[41] but have only found limited usage because there are no significant advantages associated
153 with over-sampling the absorbance spectra of blood for oximetry.

154 Multispectral oximetry models incorporating a few (typically < 10) key wavelengths have achieved
155 high quality oximetry, whilst reducing acquisition time required for spectral data acquisition. Of
156 particular note is the development of ‘snapshot’ multispectral imaging techniques where several
157 wavebands are acquired simultaneously; this avoids artefacts associated with misregistration of time-
158 sequentially recorded images.[42] The simplest form of snapshot multispectral imaging involves to
159 splitting the imaged light with an optical beam-splitter and then filter each resultant image separately
160 with bandpass filters, or by using a dichroic mirror, [4,42] however, this becomes optically inefficient
161 for large numbers of bands and problematic to implement with a single detector. Several snapshot
162 multispectral imaging devices that require only a single detector have been developed, including use
163 of a lenslet array[43] and the Image Mapping Spectrometer[44] using degmented mirrors; however to
164 date neither of these approaches have been applied extensively to oximetry. A snapshot imaging
165 system which has found significant use for oximetry is the Image Replicating Imaging Spectrometer
166 (IRIS).[11,45] This optically efficient device enables video-rate imaging at eight distinct wavebands
167 optimised for retinal oximetry. The high temporal resolution and 8 wavebands afforded by IRIS has
168 enabled several new oximetry applications, including direct observation of oxygen release by red
169 blood cells.[46]

170
171

Table 1. Retinal oximetry studies utilising multispectral imaging oximetry algorithms.

Study	Wave-range	Known parameters	Estimated parameters	Key reported OS (i.e. normal OS at normoxia - unless otherwise stated)
Schweitzer et al., (1999)[47]	510 – 586 nm 76 wavebands	ϵ , ϵ_{mel}	OS, c, d, η	A: 92.2 ± 4.1 % V: 57.9 ± 9.9 %
Drewes et al., (1999)[48]	629, 678, 821, & 899 nm.	ϵ	OS, S, c, d	A: 101 % V: 65 %
Smith et al., (2000)[49]	488, 635, 670, 752, & 830 nm	ϵ	OS, S, c, d, η	V: 42 - 56 %
Alabboud et al., (2007)[50]	500 – 700 nm 27+ wavebands	ϵ , S	OS, d, c, η	A: 96 % V: 55 %
Mordant et al., (2011)[51]	500 - 650 nm 300 wavebands	ϵ , S	OS, d, c, η	A: 104 % V: 35 %
Salzer et al., (2006)[52]	420 – 700 nm 29 wavebands	ϵ	OS, S	Arterial OS correlated well with <i>ex vivo</i> blood OS measurements
Khoobei et al., (2007)[53]	522 – 586 nm 7 wavebands	ϵ	OS	A: 92 % V: 76 %
Arimoto et al., (2010)[54]	510 – 600 nm 45 wavebands	ϵ	OS	N/A: relative OS
Furukawa et al., (2012)[54]	510 – 600 nm 7 wavebands	ϵ	OS	N/A: relative OS
Gao et al., (2012)[44]	510 - 586 nm 8 wavebands	ϵ	OS	N/A: relative OS

172
173
174
175
176

Key: A = arteries, V = veins. SO_2 = oxygen saturation, ϵ = extinction coefficient of Hb and O_2Hb , ϵ_{mel} = extinction coefficient of melanin, S = scattering contribution; c = concentration of haemoglobin, η = single/double pass contribution factor; d = diameter of vessels; K = contrast reduction factor.

178 3. BLOOD VESSELS TARGETED FOR OXIMETRY

179 3.1. Retinal oximetry

180 To date, the retinal vasculature has been the primary target for oximetry investigations in the eye.
181 The retina is a site of extremely high metabolic demand, and problems with retinal blood flow can
182 lead to a number of serious ocular conditions, including: retinal vascular occlusion[23–26] and diabetic
183 retinopathy.[13–17] Further, in ocular conditions characterised by cell loss e.g. glaucoma, estimation
184 of oxygen utilisation has provided new insights.[18–22]

185 Choroidal oximetry

186 A recent development in oximetry is the targeting of choroidal vessels for oximetry in subjects with
187 very low retinal pigmentation. The lack of retinal pigmentation allows light to traverse through the
188 retina and and dense choroidal vasculature. Kristjansdottir et al., (2013)[28] conducted an imaging
189 study of OS of choroidal blood vessels in healthy subjects; results were reported in terms of ODR
190 because ODR to OS calibration coefficients for choroidal vessels are not known and high levels optical
191 scattering prevent the use of existing oximetry models. For example, some choroidal vessels have a
192 negative optical density; i.e. they appear brighter than surrounding tissue. To date, a calibration
193 scheme for choroidal oximetry calibration has not been derived. However, this study revealed a very
194 low artery-vein difference of 4% in the choroid (instead of the typical ~30% artery-vein difference in
195 retinal vessels).[11,28] Further studies of the choroidal circulation are required to understand what
196 further physiological and clinical insights choroidal oximetry could bring.

197 3.2. Bulbar conjunctival oximetry

198 A recent oximetry study by MacKenzie et al., (2016)[32] revealed that bulbar conjunctival blood
199 vessels have oxygen dynamics that are remarkably different from any other blood vessels in the eye.
200 The bulbar conjunctival blood vessels are situated within the thin conjunctival membrane on the outer
201 surface of the sclera, and consequently are in direct contact with ambient air. This unique position of
202 the bulbar conjunctival vessels leads to oxygen diffusion occurring from air into the bulbar conjunctival
203 blood vessels. Consequently, all bulbar conjunctival blood vessels exposed to air will be highly
204 oxygenated, with little to no artery-vein difference. Study of bulbar conjunctival oxygen dynamics
205 could potentially yield insights into microvascular oxygen dynamics and related parameters. This may
206 be of particular interest for the study of oxygen dynamics in diabetes, where microvascular vessel wall
207 hardening is known to occur.[32]

208 3.3. Episcleral oximetry

209 Oximetry of the superficial episcleral blood vessels embedded into the sclera has recently been
210 achieved for the first time by MacKenzie et al (2016).[32] This study observed that when episcleral
211 vessels are exposed to a temporary hypoxic intervention, episcleral vessels dilated and episcleral OS
212 decreased. This auto-regulatory behaviour is similar to the autoregulation observed in retinal vessels
213 under similar hypoxic conditions.[11] Because episcleral vessels can be imaged on the surface of the
214 sclera, it has been suggested that episcleral vessels could be used as a proxy for retinal OS in situations
215 where retinal imaging is not feasible; e.g. in patients with cataracts. Alternatively, episcleral vessels
216 could be used as a comparison point with retinal vessels to study ocular autoregulation. Further

217 studies of episcleral vessels is required before their utility for clinically relevant oximetry can be
218 ascertained.[32]

219 **3.4. Oximetry elsewhere in the body**

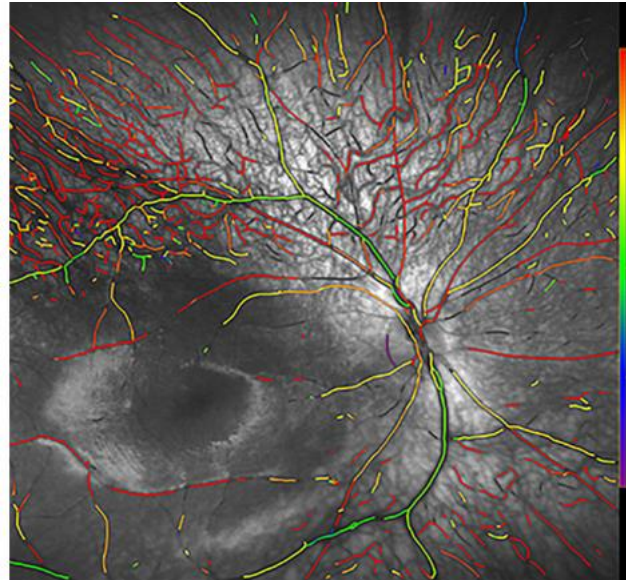
220 It is noteworthy that oximetry techniques originally developed for oximetry in the eye have
221 benefited oximetry applications elsewhere in the body. For example, multispectral imaging oximetry
222 has been employed to investigate diverse applications, including murine brain vascular oximetry,[55]
223 diabetic foot-ulcer development,[56] bowel laparoscopy,[57] skin blood flow,[58] the study of skin
224 damage due to beta radiation exposure,[59] labial, periodontal, and sublingual microvasculature,[60]
225 cancer tumour development in murine models,[39,40] and oximetry of the rat spinal cord dorsal vein
226 for studying the development of multiple sclerosis disease models.[38]

227 **4. SPECTROSCOPIC IMAGING MODALITIES FOR THE EYE**

228 The majority of oximetry studies in the eye are conducted with retinal-fundus cameras adapted for
229 two wavelength or multispectral imaging. Dual wavelength imaging can be enabled by splitting a
230 broadband retinal image with a dichroic beam-splitter, spectrally filtering the resultant images, and
231 then recording with one or more detectors.[4,31] Alternatively, wavebands may be recorded using
232 separate channels of a three-colour RGB CCD detector with additional spectral filtering to enhance
233 spectral discrimination.[9,38] The majority of multispectral and hyperspectral imaging studies have
234 employed time-sequential filtering of broadband retinal images, utilising either multiple bandpass
235 filters, a liquid-crystal tuneable filter (LCTF),[21,50,51,53,61,62] or an acousto-optic tuneable filter
236 (AOTF) for spectral discrimination.[54,63,64] LCTFs and AOTFs offer the advantages electronically-
237 controlled optical waveband switching in short timescales (~ 50 ms and 25 μ s respectively), with a
238 wide-variety of accessible wavelengths.[65] The Image Replicating Imaging Spectrometer (IRIS) has
239 enabled video-rate oximetry which has been utilised observe oxygen release by *ex vivo* red blood cells
240 upon exposure to sodium dithionite.[46,66]

241
242 Dual-wavelength scanning laser ophthalmoscopes (SLOs)[10,29,67,68] offer several advantages for
243 retinal oximetry compared to fundus cameras, including improved control of stray light, reduced
244 fundus light exposure levels, wide-field retinal scanning,[10] no requirement for pupil dilation,[68] and
245 the option to incorporate adaptive optics to compensate for eye motion and improve imaging of small
246 retinal blood vessels.[29] Recently this has enabled retinal oximetry of infants without mydriasis.⁵²
247 However, despite these advantages, SLOs are limited to available laser wavelengths, which are not
248 optimal for oximetry,[33] so further development and testing of SLO oximetry systems is required.

249
250 Slit lamps have not yet been utilised for oximetry, but could be modified for multispectral imaging.
251 The high magnification and resolution of slit lamps could enable oximetry of blood vessels as small as
252 individual capillaries and groups of red blood cells in the bulbar conjunctiva.[27]



253

254

255

256

Figure 3. Pseudo-colour OS map of retinal vessels in an infant obtained via imaging with a scanning laser ophthalmoscope. Red indicates 100% OS, purple 0% OS. Figure reproduced from Vehmeijer et al., (2016) under a Creative Commons BY license.[68]

257

258

259

260

261

262

263

264

265

266

267

268

269

Optical Coherence Tomography (OCT) is emerging as a potential retinal oximetry technology, but to date OCT oximetry has been applied only to murine models. In OCT, light backscattered from tissue is collected, and by coherence gating, is processed to form a 3D volumetric image of tissue. The ranging function of OCT provides the enhanced possibility of good control of the light paths defining optical absorption and with a reduced influence of scattering Spectroscopic Optical Coherence Tomography (S-OCT) has recently emerged as technology capable of recording 3D maps of OS with high spatial resolution. [69–71] Initially, S-OCT systems utilised the near infra-red illumination wavelengths commonly used by OCT systems. Unfortunately, near infra-red wavelengths suffer from weak optical absorption contrast between Hb and O₂Hb, resulting in sub-optimal oximetry. Consequently, newer S-OCT oximetry systems have improved oximetry capability by switching to visible wavelength illumination; visible wavelengths provide improved spectral contrast for oximetry. [72,73] However, S-OCT requires long acquisition times of up to 20 minutes for data acquisition. As such S-OCT oximetry studies have been conducted in murine models only. [74–76]

270

271

272

273

274

275

276

277

278

279

280

Photoacoustic imaging has recently emerged as a hybrid imaging modality that combines optical spectral contrast with the tissue depth penetration of ultrasound. In photoacoustic imaging, high intensity pulsed laser light (typically < 10 ns duration per pulse) is incident on the target tissue, heating the blood by less than 0.1°C and leading to rapid expansion and contraction which generates an ultrasound pulse with an amplitude proportional to the absorption of light by blood.[77] Ultrasound imaging of the emission therefore enables deep-tissue volumetric mapping of optical absorption. However, the high laser powers required for photoacoustic signal generation and requirement for ultrasonic transducer coupling to the eye make photoacoustic imaging a less attractive prospect for oximetry in the human eye compared to oximetry with fundus cameras. So far all photoacoustic studies of the eye have been limited to murine models. A good overview of photoacoustic ophthalmic imaging has been provided by Liu and Zhang (2016).[78]

281

5. VALIDATION AND TESTING OF OXIMETRY MEASUREMENTS

282 **5.1 Oxygen-sensitive challenges and interventions**

283 Oxygen-sensitive physiological challenges and interventions alter OS in subjects, allowing the
284 oximetry capability of measurement systems to be assessed, and to provide useful calibration points
285 for oximetry.[1,3,31,38,74] Further, these challenges and interventions provide physiological insights
286 into metabolism.

287 **5.1.1. Hyperoxia**

288 Perhaps the most commonly used oxygen sensitive intervention is short duration hyperoxia (i.e. an
289 excess of O₂), where a subject breathes a high O₂ (typically 100% O₂) air mixture. Hyperoxia greatly
290 increases the partial pressure of oxygen (pO₂) in blood and increases both venous and arterial OS.

291 Using the *Oxymap* system, Hardarson et al., (2006)[4] reported that retinal arterial OS is increased
292 from 96 ± 9% OS (mean ± SD) at normoxia to 101 ± 8 % OS at hyperoxia. Retinal veins experience a
293 greater increase in OS from 55 ± 14 % to 78 ± 15%.[4] Using the *Imedos* system, Hammer et al.,
294 (2008)[9] reported that retinal arterial OS increased from 98 ± 10% (mean ± SD) at normoxia to 100
295 ± 10 % at hyperoxia and that retinal venous OS increased from 65 ± 12% at normoxia to 72 ± 10 % at
296 hyperoxia.[9] Also using the *Oxymap* system, Klefter et al., (2014)[79] reported that retinal arterial OS
297 increased from 95.1 ± 5.0% (mean ± SD) at normoxia to 96.6 ± 6.4% at hyperoxia and that retinal
298 venous OS increased from 62.9 ± 6.7% at normoxia to 70.3 ± 7.8% at hyperoxia. Notably retinal and
299 veins constricted in diameter by 5.5% and 8.2%, respectively at hyperoxia compared with normoxia.
300 In all cases the increase in retinal venous OS was greater than the increase in retinal arterial OS.

301 A hyperoxia intervention was used by Krisjandottir et al., (2013)[28] to show that all choroidal
302 vessels are highly oxygenated at normoxia; this could only have been achieved with a hyperoxia
303 intervention because two-wavelength oximetry calibration has not yet been demonstrated for
304 choroidal vessels.[28]

305 **5.1.2. Hypoxia**

306 An alternative OS-sensitive intervention is acute mild hypoxia, where systematic OS is decreased
307 by subjects inhaling a hypoxic air mixture (typically ~ 15% O₂) for several minutes. The 10 - 15 % OS
308 decrease induced by acute mild hypoxia studies is similar in magnitude to the decrease in OS
309 experience in high-altitude airplane travel [80] and thus can be considered safe in healthy subjects for
310 short durations.

311 Choudhary et al., (2013)[11] investigated the auto-regulatory effects of acute mild hypoxia in
312 retinal vessels. OS was observed to decrease for both arterioles and venules but artery-vein (AV) OS
313 difference remained constant. Both retinal arteries and veins were observed to dilate under hypoxia,
314 with arteries showing a larger increase.[11] This provided new insight into the interplay between the
315 vascular and choroidal oxygen supplies in the retina and auto-regulatory responses.

316 MacKenzie et al., (2016)[32] utilised a similar hypoxia intervention to study bulbar conjunctival and
317 episcleral oxygen dynamics. Episcleral vessels were observed to behave similarly to retinal vessels
318 under acute mild hypoxia, but episcleral arteries and veins were not distinguished. However, hypoxic
319 bulbar conjunctival vessels were observed to re-oxygenate to high OS via oxygen diffusion when
320 exposed to ambient air. This effect would not have been possible to observe without the hypoxic
321 intervention.[32]

322 Severe graded hypoxia to as low as 9% O₂ was used by Yi et al., (2015)[74] to investigate the
323 metabolic response of the rat retina to hypoxia, finding that the metabolic demand of the retina is
324 increased at hypoxia.[74]

325 **5.1.3. Retinal light exposure**

326 Retinal light exposure is known to alter retinal metabolic demand, thus inducing an autoregulation
327 effect, and thus altering retinal OS. Using the *Oxymap* system, Hardarson et al., (2009)[8] found that
328 retinal OS of both arteries and veins is higher in for an eye not exposed to light than for an eye exposed
329 to light.[8] With the *Imedos* system, Hammer et al., (2011)[6] found that retinal venous OS increased
330 by an average of ~ 5% after ~ 100s of 12.5 Hz flicker stimulation. In contrast, retinal arterial OS
331 decreased slightly on average by ~ 1%. The diameter of both arteries and veins increased significantly,
332 indicating increased blood flow. A later study by Hammer et al., (2012)[7] that compared diabetic
333 patients to healthy controls found that venous OS of diabetic patients increased less under flicker
334 stimulation than the change observed in healthy controls.[7] Similarly, venous dilation was less for
335 diabetic patients than healthy controls. This suggests that retinal blood flow regulation is impaired in
336 diabetic patients.[7]

337 **5.2. Eye-mimicking *ex vivo* oximetry phantoms**

338 Oximetry can be validated using *ex vivo* blood of various OS levels in *in vitro* phantoms that mimic
339 blood vessels within the eye. Various strategies to phantom design and construction have been
340 implemented.

341 Lemaillet et al., (2009)[81] developed a multi-layered dynamic eye phantom, incorporating flowing
342 blood to simulate *in vivo* blood flow. Flowing blood is known to have different reflectance and
343 scattering parameters than static blood due to alignment of red blood cells in laminar flow
344 conditions.[82,83] The phantom consisted of: a plano-convex lens to mimic the human lens, a choroid
345 mimicking layer, and a layer mimicking the retinal pigment endothelium. A 100 µm capillary was
346 supplied with flowing bovine blood from a reservoir, and OS was modified by adding sodium
347 hydrosulphide to deoxygenate blood, with additional oxygen supplied via a fuel cell to the blood
348 reservoir. It was noted that construction of this phantom was highly time consuming.[81]

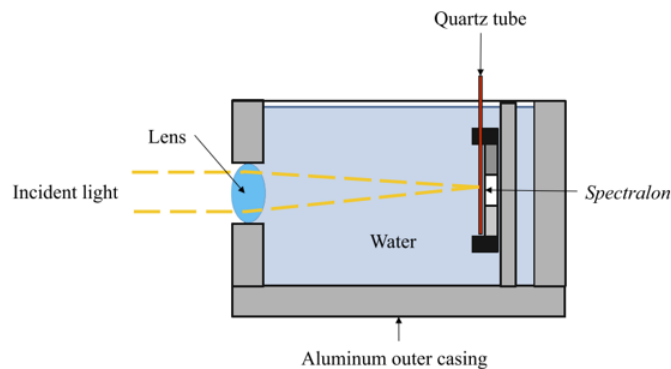
349 Mordant et al., (2011)[62] constructed a simple model eye consisting of straight quartz capillaries
350 of various inner diameters (50, 100, and 150 µm) filled with static human blood (see Figure 4). A convex
351 lens mimicked the human lens and distilled water mimicked the vitreous humour. A white diffuse
352 reflectance material - *Spectralon*[™] - mimicked the scleral back-reflectance.[30,84] Blood OS was varied
353 by placing samples in air mixtures with varied fractions of O₂ and OS was confirmed with a blood gas
354 analyser.[62] This phantom was used to validate later *in vivo* oximetry studies.[51]

355 MacKenzie et al., (2016)[32] constructed a simple sclera-mimicking phantom for bulbar
356 conjunctival and episcleral oximetry. This phantom consisted of a 100 µm FEP plastic capillary above
357 a *Spectralon*[™] backing. The capillary was filled with flowing *ex vivo* equine blood and OS was varied by
358 addition of sodium dithionite[66]; OS was confirmed with a blood gas analyser. Whilst not
359 sophisticated, this phantom was sufficient for oximetry validation.[32]

360 Recently, Ghassemi et al., (2015)[85,86] have reported a bio-mimicking phantom designed from
361 real retinal blood vessel patterns. These phantoms are 3D printed from a photoreactive resin in a
362 pattern based up a 3D sectioned image of retinal vessels. A commercially available O₂Hb solution was

363 used in place of whole blood. Yeast was used to consume oxygen in the solution, with OS decreasing
364 over time.[85] Bio-mimicking phantoms may be advantageous in future because they could simulate
365 realistic blood flow patterns and thus reproduce features like laminar flow seen in branching retinal
366 veins.[42]

367 Corcoran et al., (2014)[87] created an advanced, wide-field spherical eye with 3D-printed phantom
368 retina, an optics based on a rigorous schematic eye model. The retina incorporated embedded image
369 resolution test targets and simulated retinal tissue layers. This style of advanced phantom has not yet
370 been applied to oximetry, but could be highly beneficial in future studies that more closely resemble
371 *in vivo* applications.[87]



372
373 **Figure 4.** Diagram of a model eye phantom used by Mordant et al., (2011)[62] to validate
374 oximetry capability of a hyperspectral imaging system. Figure reproduced with
375 permission.

376 6. CLINICAL INSIGHTS

377

378 6.1. Diabetic retinopathy

379

380 Diabetic retinopathy is an important potentially blinding eye condition, which can affect patients
381 in the working-age population. Diabetic retinopathy causes loss of capillaries in the retinal circulation,
382 and visual loss can occur following the resultant retinal ischaemia, production of vaso-proliferative
383 substances e.g. vascular endothelial growth factor (VEGF), and then misdirected growth of new
384 vessels, which are fragile, and ultimately result in vitreous haemorrhage and/or retinal detachment.
385 Diabetic visual loss can also follow leakage from retinal vessels close to the macula causing macular
386 oedema. Research has explored the use of retinal oximetry to detect the effects on arterial and venous
387 oxygen saturation of diabetic retinopathy. Early work by Beach et al. detailed acute changes in retinal
388 oxygen utilisation with hyperglycaemia.[13] Later work, using dual-wavelength oximetry has
389 demonstrated that higher venous oxygen saturation is associated with established diabetic
390 retinopathy,[17] which, in some studies shows a dose-related relationship with increasing severity of
391 proliferative diabetic retinopathy.[15,16] These observations might represent the formation of
392 arterio-venous shunts in the retinal circulation to circumvent the capillary loss, or, alternatively, might
393 simply represent reduced oxygen utilisation by pathologically atrophic inner retinal cellular elements.
394 Elevated venous saturation in patients with diabetic retinopathy may be a clinically useful measure of
395 underlying retinal ischaemia, and may become an indicator of the need for retinal photocoagulation

396 treatment. Interestingly, application of retinal photocoagulation has not been shown to result in any
397 significant changes in venous retinal OS.[15]

398

399 **6.2. Retinal vessel occlusion**

400

401 Retinal venous occlusion is an important cause of visual morbidity in older patients with general
402 vascular risk factors, e.g. hypertension. The pathological effects of a central retinal vein occlusion may
403 include retinal ischaemia, production of VEGF, and growth of new vessels, which can cause visual loss
404 from vitreous haemorrhage, or neo-vascular glaucoma. Retinal oximetry research has been directed
405 at detecting OS abnormalities. Such abnormalities might provide early evidence of retinal ischemia,
406 and thus enable treatment to be applied at an earlier stage; hopefully reducing the risk of the patient
407 developing neo-vascular glaucoma. Dual-wavelength oximetry research studies in central retinal
408 venous occlusion have consistently shown lower levels of venous OS, consistent with generalised
409 retinal ischaemia.[24, 25] Studies in partial, or branch, retinal occlusion have shown variable results,
410 with sometimes increased, and sometimes reduced venous saturations. This may reflect the different,
411 localised impact of a venous occlusion, and/or the maturity of the occlusion, as well as the impact of
412 local homeostatic mechanisms.[23,26] Central retinal artery occlusion has been noted to result in
413 severe retinal hypoxia, with low arteriovenous difference, suggesting cell death.

414

415 **6.3. Glaucoma**

416

417 Glaucoma is a common cause of blindness in older patients, and a family history of glaucoma is an
418 important risk factor. The diagnosis of glaucoma rests on detection of characteristic changes at the
419 optic nerve head which are associated with visual field loss. Many, but not all, patients with glaucoma
420 will have elevated intraocular pressure. The pathological change, which ultimately results in visual loss
421 is retinal ganglion cell axon loss, which essentially results in atrophy of the cellular elements of the
422 inner retina. Oximetry studies have investigated the changes in oxygen consumption within the retinal
423 circulation that are associated with the cellular loss. Research work using both dual wavelength and
424 multispectral imaging has demonstrated elevated venous saturation, with some studies showing
425 increasingly elevated venous saturation in more severely affected eyes.[18–22] These studies suggest
426 a role for retinal oximetry as a means to estimate inner retinal oxygen consumption in glaucoma and
427 other optic neuropathies. Further research is required to investigate whether interventions to lower
428 the intraocular pressure might demonstrate reversible changes in oxygen utilisation, which could be
429 a favourable prognostic outcome from the intervention.

430

431 **7. EXPERT COMMENTARY**

432 Oximetry in the eye has revealed a great deal about physiological norms and autoregulation in the
433 retina. However, there is still considerable insight to be gleaned in application of oximetry to choroidal,
434 episcleral, and bulbar conjunctival blood vessels. OS norms of these vessel beds require further study,
435 and may provide insights into disease development and treatment.

436

437 The advent of commercially available retinal oximetry systems, i.e. the *Oxymap* and *Imedos*
438 systems have enabled retinal oximetry in the clinic, which has allowed studies of many retinal diseases
439 with increasing statistical power. Clinical studies hold the potential to provide deeper insight into

440 disease development and treatment of conditions such as diabetic retinopathy,[13–17] glaucoma,[18–
441 22] and retinal vessel occlusion.[23–26]

442

443 The use of oxygen-sensitive interventions such as hyperoxia, hypoxia, and retinal light exposure
444 have been able to compliment oximetry measurements on provide comparative intervention tests. In
445 the retina a flicker intervention has enabled comparisons of the metabolic response of healthy control
446 subjects and patients with diabetic retinopathy.[6] Notably, oxygen-sensitive interventions have
447 enabled insight into the fundamental physiology of oxygen supply to the choroidal vessels,[28]
448 episcleral circulation, and bulbar conjunctival circulation.[27] There is much potential in investigating
449 these new targets for oximetry.

450

451 The development of new technology and innovation in image processing is also helping to drive
452 new oximetry applications that were not previously possible. With improved techniques, oximetry is
453 now possible in small retinal vessels,[29] in the choroid,[28] in the episcleral and bulbar conjunctival
454 vessels,[32] and in the retina of infants.[68] New applications will invariably find new insights into the
455 eye which are fundamentally and clinically important.

456

457 One of the fundamental challenges for oximetry is validation of measurements. Arterial OS can be
458 compared to invasive blood gas measurements or pulse oximetry. However, venous calibration is
459 extremely challenging, and is influenced by blood vessel diameter and fundus pigmentation.[9,31]
460 Multispectral algorithms offer a ‘calibration free’ oximetry method, but accurate validation is still
461 highly challenging due to the complex optical environment of the eye. Validation with *ex vivo* blood is
462 also complicated by numerous factors including blood aggregation, red blood cell death, alignment of
463 red blood cells under flow, and imperfect phantoms.[12,51,81]

464

465 **Five-year view**

466 In the last five years, oximetry has revealed the fundamental physiology of OS in episcleral
467 vessels,[27] the bulbar conjunctival vessels,[27] and the choroidal circulation.[28] The physiology
468 understanding of these vessel beds has been enabled by the development of hyperoxia and hypoxia
469 OS-sensitive interventions.

470 Application of oximetry to the eye is continuing to yield fresh insight into the physiology of the eye
471 and ocular disease development, and treatment. Commercially available two-wavelength oximetry
472 systems have enabled oximetry in the clinic and studies of diseases such as diabetic retinopathy, vessel
473 occlusion, and glaucoma have resulted. In the next five years, oximetry will likely be applied to
474 increasingly diverse disease applications.

475 Imaging technology and imaging analysis is also continuing to develop, pushing new boundaries in
476 spatial and temporal resolution. This can enable oximetry in new applications, such as the study of
477 small retinal vessels,[29] oximetry in infants,[68] in *ex vivo* red blood cells.[46] The advent of 3D
478 printing has allowed the development of bio-mimicking phantoms[87] based on real blood vessel
479 network patterns,[85] enabling the study of blood flow in realistic yet controlled scenarios. The fast
480 paced development of 3D printing makes this field of phantom development particularly promising.

481 **Key issues**

- 482 ▪ Spectroscopic oximetry is most widely applied to the study of the retinal circulation, but
483 oximetry of the bulbar conjunctival, episcleral, and choroidal circulations has also recently
484 emerged.
- 485 ▪ Oxygen-sensitive interventions such as hyperoxia, hypoxia, and retinal flicker illumination
486 provide oximetry validation, clinical insights, and have revealed fundamental physiology of
487 the choroid, the episcleral vessels, and the bulbar conjunctival vessels.
- 488 ▪ Commercial oximetry systems have enabled clinical studies in individual patients and in larger
489 group studies, enabling deeper understanding of the development and treatment of diseases
490 such as diabetes, retinal vessel occlusion, and glaucoma.
- 491 ▪ Development of new imaging capabilities, advanced image processing concepts, and ever-
492 improving phantom development are continuing to push new oximetry applications and
493 enable fresh insights into the physiology of the eye.
- 494

495 **7. CONCLUSIONS**

496 Oximetry has enabled many insights in the fundamental physiology and oxygen dynamics of the
497 eye. In particular, oximetry has enabled the study of retinal autoregulation, retinal disease
498 development, and retinal disease treatment. Recently, the fundamental oxygen dynamics of the
499 bulbar conjunctiva, the episcleral vessels, and the choroid have been revealed by oximetry combined
500 with complimentary OS-sensitive hyperoxia and hypoxia interventions.

501 Commercially available retinal oximetry systems have enabled oximetry in the clinic, allowing
502 studies of retinal OS in many diseases and treatments. In particular, diabetic retinopathy, retinal
503 vascular occlusion, and glaucoma. Oxygen sensitive interventions - such as retinal flicker illumination,
504 hypoxia, and hyperoxia - have provided means to validate oximetry, establish physiological norms,
505 and probe auto-regulation responses.

506 The predominant imaging systems in the field of retinal oximetry are based upon modified retinal-
507 fundus cameras, however SLO-based systems show considerable promise with a comparatively larger
508 field of view, the potential for improved spatial and depth resolution and accuracy. Further, SLOs
509 require no mydriasis. Yet, existing SLO systems are limited to commercially favoured laser
510 wavelengths, and as such may provide sub-optimal oximetry measurements. Confocal SLOs offer
511 potential for improved accuracy through improved control of stray light and the longer effect path
512 lengths enable good oximetric contrast with a wide range of low-cost infrared lasers, although optical
513 efficiency is necessarily lower. Further development of SLO oximetry systems is a particularly fertile
514 area.

515 New oximetry applications are currently emerging, namely oximetry of the small retinal vessels,
516 retinal oximetry in infants, and oximetry of the bulbar conjunctiva, episcleral, and choroidal vessels.
517 These new applications for oximetry will enable researchers to understand the OS in physiological
518 norms and disease across multiple ocular blood vessel beds.

519

520 **BIBLIOGRAPHY**

- 521 1. Hickam JB, Sieker HO, Frayser R. Studies of retinal circulation and A-V oxygen difference in man.
522 *Trans. Am. Clin. Climatol. Assoc.* 71(657), 34–44 (1959).
- 523 2. Hickam JB, Frayser R, Ross JC. A study of retinal venous blood oxygen saturation in human
524 subjects by photographic means. *Circulation.* 27(3), 375–385 (1963).
- 525 3. Hickam JB, Frayser R. Studies of the retinal circulation in man. Observations on vessel diameter,
526 arteriovenous oxygen difference, and mean circulation time. *Circulation.* XXXIII(February),
527 302–316 (1966).
- 528 4. Hardarson SH, Harris A, Karlsson RA, *et al.* Automatic retinal oximetry. *Invest. Ophthalmol. Vis. Sci.*
529 47(11), 5011–6 (2006).
- 530 5. Beach J. Pathway to retinal oximetry. *Transl Vis Sci Technol.* 3(5), 1–9 (2014).
- 531 6. Hammer M, Vilser W, Riemer T, *et al.* Retinal venous oxygen saturation increases by flicker light
532 stimulation. *Invest. Ophthalmol. Vis. Sci.* 52(1), 274–7 (2011).
- 533 7. Hammer M, Heller T, Jentsch S, *et al.* Retinal vessel oxygen saturation under flicker light
534 stimulation in patients with nonproliferative diabetic retinopathy. *Invest. Ophthalmol. Vis. Sci.*
535 53(7), 4063–8 (2012).
- 536 8. Hardarson SH, Basit S, Jonsdottir TE, *et al.* Oxygen saturation in human retinal vessels is higher
537 in dark than in light. *Invest. Ophthalmol. Vis. Sci.* 50(5), 2308–11 (2009).
- 538 9. Hammer M, Vilser W, Riemer T, Schweitzer D. Retinal vessel oximetry-calibration,
539 compensation for vessel diameter and fundus pigmentation, and reproducibility. 13(5), 1–7
540 (2008).
- 541 10. Kristjansdottir JV, Hardarson SH, Halldorsson GH, Karlsson RA, Eliasdottir TS, Stefánsson E.
542 Retinal oximetry with a scanning laser ophthalmoscope. *Investig. Ophthalmology Vis. Sci.* 55(5),
543 3120 (2014).
- 544 11. Choudhary TR, Ball D, Fernandez Ramos J, McNaught AI, Harvey AR. Assessment of acute mild
545 hypoxia on retinal oxygen saturation using snapshot retinal oximetry. *Invest. Ophthalmol. Vis. Sci.*
546 54(12), 38–43 (2013).
- 547 12. MacKenzie LE. Oximetry of bulbar conjunctival and episcleral microvasculature using snapshot
548 multispectral imaging. *Retin. Oximetry Work.* 2016. (2016).
- 549 13. Tiedeman JS, Kirk SE, Srinivas S, Beach JM. Retinal oxygen consumption during hyperglycemia
550 in patients with diabetes without retinopathy. *Ophthalmology.* 105(1), 31–36 (1998).
- 551 14. Jørgensen CM, Hardarson SH, Bek T. The oxygen saturation in retinal vessels from diabetic
552 patients depends on the severity and type of vision-threatening retinopathy. *Acta Ophthalmol.*
553 92(1), 34–39 (2014).
- 554 15. Jørgensen C, Bek T. Increasing oxygen saturation in larger retinal vessels after
555 photocoagulation for diabetic retinopathy. *Investig. Ophthalmol. Vis. Sci.* 55(8), 5365–5369
556 (2014).
- 557 16. Hammer M, Vilser W, Riemer T, *et al.* Diabetic patients with retinopathy show increased retinal
558 venous oxygen saturation. *Graefes Arch. Clin. Exp. Ophthalmol.* 247(8), 1025–30 (2009).
- 559 17. Hardarson SH, Stefánsson E. Retinal oxygen saturation is altered in diabetic retinopathy. *Br. J.*
560 *Ophthalmol.* 96(4), 560–3 (2012).

- 561 18. Olafsdottir OB, Hardarson SH, Gottfredsdottir MS, Harris A, Stefánsson E. Retinal oximetry in
562 primary open-angle glaucoma. *Invest. Ophthalmol. Vis. Sci.* 52(9), 6409–13 (2011).
- 563 19. Olafsdottir, OB Vandewalle E, Abegão, Pinto L Geirsdottir A, De Clerck E, *et al.* Retinal oxygen
564 metabolism in healthy subjects and glaucoma patients. *Br. J. Ophthalmology.* 98(3), 329–33
565 (2014).
- 566 20. Vandewalle E, Pinto LA, Olafsdottir OB, *et al.* Oximetry in glaucoma: Correlation of metabolic
567 change with structural and functional damage. *Acta Ophthalmol.* 92(2), 105–110 (2014).
- 568 21. Mordant DJ, Al-Abboud I, Muyo G, Gorman A, Harvey AR, McNaught AI. Oxygen saturation
569 measurements of the retinal vasculature in treated asymmetrical primary open-angle
570 glaucoma using hyperspectral imaging. *Eye.* 28(10), 1190–200 (2014).
- 571 22. Boeckeaert J, Vandewalle E, Stalmans I. Oximetry: recent insights into retinal vasopathies and
572 glaucoma. *Bull. Soc. Belge Ophthalmol.* (319), 75–83 (2012).
- 573 23. Hardarson SH, Stefánsson E. Oxygen saturation in branch retinal vein occlusion. *Acta*
574 *Ophthalmol.* 90(5), 466–470 (2012).
- 575 24. Hardarson SH, Elfarsson A, Agnarsson BA, Stefansson E. Retinal oximetry in central retinal
576 artery occlusion. *Acta Ophthalmol.* 91(2), 189–190 (2013).
- 577 25. Eliasdottir TS, Bragason D, Hardarson SH, Kristjansdottir G, Stefánsson E. Venous oxygen
578 saturation is reduced and variable in central retinal vein occlusion. *Graefe's Arch. Clin. Exp.*
579 *Ophthalmol.* (2014).
- 580 26. Lin L-L, Dong Y-M, Zong Y, *et al.* Study of retinal vessel oxygen saturation in ischemic and non-
581 ischemic branch retinal vein occlusion. *Int. J. Ophthalmol.* 9(1), 99–107 (2016).
- 582 27. MacKenzie LE, Choudhary TR, McNaught AI, Harvey AR. In vivo oximetry of human bulbar
583 conjunctival and episcleral microvasculature using snapshot multispectral imaging. *Exp. Eye*
584 *Res.* 149, 48–58 (2016).
- 585 28. Kristjansdottir JV, Hardarson SH, Harvey AR, Olafsdottir OB, Eliasdottir TS, Stef E. Choroidal
586 oximetry with a noninvasive spectrophotometric oximeter. *Invest. Ophthalmol. Vis. Sci.* 54(5),
587 3234–3239 (2013).
- 588 29. Li H, Lu J, Shi G, Zhang Y. Measurement of oxygen saturation in small retinal vessels with
589 adaptive optics confocal scanning laser ophthalmoscopy. *JBO Lett.* 16(11) (2011).
- 590 30. Hammer M, Leistritz S, Leistritz L, Schweitzer D. Light paths in retinal vessel oxymetry. *IEEE*
591 *Trans. Biomed. Eng.* 48(5), 592–8 (2001).
- 592 31. Beach JM, Schwenzer KJ, Srinivas S, Kim D, Tiedeman JS. Oximetry of retinal vessels by dual-
593 wavelength imaging: calibration and influence of pigmentation. *JAP.* 86(2), 748–758 (1999).
- 594 32. MacKenzie LE, Choudhary TR, McNaught AI, Harvey AR. In vivo oximetry of human bulbar
595 conjunctival and episcleral microvasculature using snapshot multispectral imaging. *Exp. Eye*
596 *Res.* 149, 48–58 (2016).
- 597 33. Smith MH. Optimum wavelength combinations for retinal vessel oximetry. *Appl. Opt.* 38(1),
598 258–267 (1999).
- 599 34. Mackenzie LE. In vivo microvascular oximetry using multispectral imaging. Chapter 5: Rat spinal
600 cord oximetry. (November) (2016).
- 601 35. Pittman R, Duling B. A new method for the measurement of percent oxyhemoglobin. *J. Appl.*

- 602 *Physiol.* 38(2) (1975).
- 603 36. Delori FC. Noninvasive technique for oximetry of blood in retinal vessels. *Appl. Opt.* 27(6),
604 1113–1125 (1988).
- 605 37. Delori FC. Spectrophotometer for noninvasive measurement of intrinsic fluorescence and
606 reflectance of the ocular fundus. *Appl. Opt.* 33(31), 7439–7452 (1994).
- 607 38. van der Putten MA, MacKenzie LE, Davies AL, *et al.* A multispectral microscope for in vivo
608 oximetry of rat dorsal spinal cord vasculature. *Physiol. Meas.* (2016).
- 609 39. Sorg BS, Moeller BJ, Donovan O, Cao Y, Dewhirst MW. Hyperspectral imaging of hemoglobin
610 saturation in tumor microvasculature and tumor hypoxia development. *J. Biomed. Opt.* 10(4),
611 44004 (2005).
- 612 40. Sorg BS, Hardee ME, Agarwal N, Moeller BJ, Dewhirst MW. Spectral imaging facilitates
613 visualization and measurements of unstable and abnormal microvascular oxygen transport in
614 tumors. *J. Biomed. Opt.* 13(1), 14026 (2008).
- 615 41. Hammer M, Schweitzer D. Quantitative reflection spectroscopy at the human ocular fundus.
616 *Phys. Med. Biol.* 47(2), 179–91 (2002).
- 617 42. Hendargo HC, Zhao Y, Allenby T, Palmer GM. Snap-shot multispectral imaging of vascular
618 dynamics in a mouse window-chamber model. *Opt. Lett.* 40(14), 3292–3295 (2015).
- 619 43. Ramella-Roman JC, Mathews SA. Spectroscopic measurements of oxygen saturation in the
620 retina. *IEEE J. Sel. Top. Quantum Electron.* 13(6), 1697–1703 (2007).
- 621 44. Gao L, Smith RT, Tkaczyk TS. Snapshot hyperspectral retinal camera with the Image Mapping
622 Spectrometer (IMS). *Biomed. Opt. Express.* 3(1), 48–54 (2012).
- 623 45. Gorman AS. Snapshot spectral imaging using image replication and birefringent
624 interferometry: principles and applications. (2010).
- 625 46. Fernandez Ramos J, Brewer LR, Gorman A, Harvey AR. Video-rate multispectral imaging:
626 application to microscopy and macroscopy. In: *Classical Optics 2014, OSA Technical Digest.*
627 Optical Society of America, Washington, D.C. (2014).
- 628 47. Schweitzer D, Hammer M, Kraft J, Thamm E, Königsdörffer E, Strobel J. In vivo measurement of
629 the oxygen saturation of retinal vessels in healthy volunteers. *IEEE Trans. Biomed. Eng.* 46(12),
630 1454–65 (1999).
- 631 48. Drewes J, Smith M, Hiliman L, *et al.* Instrument for the measurement of retinal vessel oxygen
632 saturation. *BiOS'99 Int. Biomed. Opt. Symp. Int. Soc. Opt. Photonics.* 3591(January), 114–120
633 (1999).
- 634 49. Smith MH, Denninghoff KR, Lompando A, Hillman LW. Retinal vessel oximetry: toward absolute
635 calibration. *Proc. SPIE.* 3908, 217–226 (2000).
- 636 50. Alabboud I, Muyo G, Gorman A, *et al.* New spectral imaging techniques for blood oximetry in
637 the retina. *Proc. SPIE 6631, Nov. Opt. Instrum. Biomed. Appl. III.* 6631 (2007).
- 638 51. Mordant DJ, Al-Abboud I, Muyo G, *et al.* Spectral imaging of the retina. *Eye.* 25(3), 309–20
639 (2011).
- 640 52. Salyer DA, Beaudry N, Basavanthappa S, *et al.* Retinal oximetry using intravitreal illumination.
641 *Curr. Eye Res.* 31(7–8), 617–27 (2006).
- 642 53. Khoobehi B, Ning J, Puissegur E, Bordeaux K, Balasubramanian M, Beach J. Retinal oxygen

- 643 saturation evaluation by multi-spectral fundus imaging. 6511, 65110B–65110B–6 (2007).
- 644 54. Arimoto H, Furukawa H. Retinal oximetry with 510 - 600 nm light based on partial least-squares
645 regression technique. *Jpn. J. Appl. Phys.* 49(11) (2010).
- 646 55. Shonat RD, Wachman S. Near-simultaneous hemoglobin saturation and oxygen tension maps
647 in mouse brain using an AOTF microscope. *Biophys. J.* 73(September), 1223–1231 (1997).
- 648 56. Yudovsky D, Nouvong A, Schomacker K, Pilon L. Assessing diabetic foot ulcer development risk
649 with hyperspectral tissue oximetry. *J. Biomed. Opt.* 16(2), 26009 (2011).
- 650 57. Clancy NT, Arya S, Stoyanov D, Singh M, Hanna GB, Elson DS. Intraoperative measurement of
651 bowel oxygen saturation using a multispectral imaging laparoscope. *Biomed. Opt. Express.*
652 6(10), 4179–90 (2015).
- 653 58. Gupta N, Ramella-Roman JC. Detection of blood oxygen level by noninvasive passive spectral
654 imaging of skin. *Proc. SPIE.* 6842, 68420C–68420C–8 (2008).
- 655 59. Chin MS, Freniere BB, Lo Y-C, *et al.* Hyperspectral imaging for early detection of oxygenation
656 and perfusion changes in irradiated skin. *J. Biomed. Opt.* 17(2), 26010 (2012).
- 657 60. Townsend D, D’Aiuto F, Deanfield J. *In Vivo* Capillary Loop Hemoglobin Spectroscopy in Labial,
658 Sublingual, and Periodontal Tissues. *Microcirculation.* 22(6), 475–484 (2015).
- 659 61. Hirohara Y, Okawa Y, Mihashi T, *et al.* Validity of retinal oxygen saturation analysis:
660 hyperspectral imaging in visible wavelength with fundus camera and liquid crystal wavelength
661 tunable filter. *Opt. Rev.* 14(3), 151–158 (2007).
- 662 62. Mordant DJ, Al-Abboud I, Muyo G, *et al.* Validation of human whole blood oximetry, using a
663 hyperspectral fundus camera with a model eye. *Invest. Ophthalmol. Vis. Sci.* 52(5), 2851–9
664 (2011).
- 665 63. Furukawa H, Arimoto H, Shirai T, Ooto S, Hangai M, Yoshimura N. Oximetry of retinal capillaries
666 by multicomponent analysis. *Appl. Spectrosc.* 66(8), 962–969 (2012).
- 667 64. Patel SR, Flanagan JG, Shahidi AM, Sylvestre JP, Hudson C. A prototype hyperspectral system
668 with a tunable laser source for retinal vessel imaging. *Investig. Ophthalmol. Vis. Sci.* 54(8),
669 5163–5168 (2013).
- 670 65. Levenson R. Spectral imaging in biomedicine: A selective overview. *Proc. SPIE.* 3438, 300–312
671 (1998).
- 672 66. Briley-Saebo K, Bjornerud A. Accurate de-oxygenation of ex vivo whole blood using sodium
673 dithionite. *Proc. Intl. Soc. Mag. Reson. Med.* 8, 2025 (2000).
- 674 67. Ashman RA, Reinholz F, Eikelboom RH. Oximetry with a multiple wavelength SLO. *Int.*
675 *Ophthalmol.* 23(4–6), 343–346 (2001).
- 676 68. Vehmeijer WB, Magnúsdóttir V, Elíasdóttir TS, Hardarson SH, Schalijs-Delfos NE, Stefánsson E.
677 Retinal Oximetry with Scanning Laser Ophthalmoscope in Infants. *PLoS One.* 11(2), e0148077
678 (2016).
- 679 69. Faber DJ, van Leeuwen TG. Are quantitative attenuation measurements of blood by optical
680 coherence tomography feasible? *Opt. Lett.* 34(9), 1435–1437 (2009).
- 681 70. Lu C-W, Lee C-K, Tsai M-T, Wang Y-M, Yang CC. Measurement of the hemoglobin oxygen
682 saturation level with spectroscopic spectral-domain optical coherence tomography. *Opt. Lett.*
683 33(5), 416–8 (2008).

- 684 71. Kagemann L, Wollstein G, Wojtkowski M, *et al.* Spectral oximetry assessed with high-speed
685 ultra-high-resolution optical coherence tomography. *J. Biomed. Opt.* 12(4) (2007).
- 686 72. Robles FE, Chowdhury S, Wax A. Assessing hemoglobin concentration using spectroscopic
687 optical coherence tomography for feasibility of tissue diagnostics. *Biomed. Opt. Express.* 1(1),
688 310–317 (2010).
- 689 73. Yi J, Li X. Estimation of oxygen saturation from erythrocytes by high-resolution spectroscopic
690 optical coherence tomography. *Opt. Lett.* 35(12), 2094–6 (2010).
- 691 74. Yi J, Liu W, Chen S, *et al.* Visible light optical coherence tomography measures retinal oxygen
692 metabolic response to systemic oxygenation. *Light Sci. Appl.* 4(9), e334 (2015).
- 693 75. Chen S, Yi J, Zhang HF. Measuring oxygen saturation in retinal and choroidal circulations in rats
694 using visible light optical coherence tomography angiography. *Biomed. Opt. Express.* 6(8), 2840
695 (2015).
- 696 76. Chong SP, Merkle CW, Leahy C, Radhakrishnan H, Srinivasan VJ. Quantitative microvascular
697 hemoglobin mapping using visible light spectroscopic Optical Coherence Tomography. *Biomed.*
698 *Opt. Express.* 6(4), 1429 (2015).
- 699 77. Beard P. Biomedical photoacoustic imaging. *Interface Focus.* 1(4), 602–31 (2011).
- 700 78. Liu W, Zhang HF. Photoacoustic imaging of the eye : a mini review. *Biochem. Pharmacol.* (2016).
- 701 79. Klefter ON, Lauritsen AØ, Larsen M. Retinal hemodynamic oxygen reactivity assessed by
702 perfusion velocity, blood oximetry and vessel diameter measurements. *Acta Ophthalmol.* , 1–
703 10 (2014).
- 704 80. Humphreys S, Deyermond R, Bali I, Stevenson M, Fee JPH. The effect of high altitude
705 commercial air travel on oxygen saturation. *Anaesthesia.* 60(5), 458–60 (2005).
- 706 81. Lemaillot P, Ramella-Roman JC. Dynamic eye phantom for retinal oximetry measurements. *J.*
707 *Biomed. Opt.* 14(6) (2009).
- 708 82. Klose HJ, Volger E, Brechtelsbauer H, Heinich L, Schmid-Schönbein H. Microrheology and light
709 transmission of blood. *Pflügers Arch. - Eur. J. Physiol.* 333(2), 126–139 (1972).
- 710 83. Hammer M, Schweitzer D, Michel B, Thamm E, Kolb a. Single scattering by red blood cells.
711 *Appl. Opt.* 37(31), 7410–7418 (1998).
- 712 84. Rodmell PI, Crowe JA, Gorman A, *et al.* Light path-length distributions within the retina. *J.*
713 *Biomed. Opt.* 19(3), 36008 (2014).
- 714 85. Ghassemi P, Wang J, Melchiorri AJ, *et al.* Rapid prototyping of biomimetic vascular phantoms
715 for hyperspectral reflectance imaging. *J. Biomed. Opt.* 20(12), 121312 (2015).
- 716 86. Wang J, Ghassemi P, Melchiorri A, *et al.* 3D printed biomimetic vascular phantoms for
717 assessment of hyperspectral imaging systems. *Des. Perform. Valid. Phantoms Used Conjunction*
718 *with Opt. Meas. Tissue VII, Proc. SPIE.* 9325 (2015).
- 719 87. Corcoran A, Muyo G, van Hemert J, Gorman A, Harvey AR. Application of a wide-field phantom
720 eye for optical coherence tomography and reflectance imaging. *J. Mod. Opt.* 62(21), 1828–1838
721 (2015).

722 **Financial and competing interests**

723 The authors report no conflicts of interest.